Face Recognition with Temporal Invariance: A 3D Aging Model

Unsang Park, Yiying Tong and Anil K. Jain
Michigan State University
East Lansing, MI 48824, USA
{parkunsa,ytong,jain}@cse.msu.edu

Abstract

The variation caused by aging has not received adequate attention compared with pose, lighting, and expression variations. Aging is a complex process that affects both the 3D shape of the face and its texture (e.g., wrinkles). While the facial age modeling has been widely studied in computer graphics community, only a few studies have been reported in computer vision literature on age-invariant face recognition. We propose an automatic aging simulation technique that can assist any existing face recognition engine for aging-invariant face recognition. We learn the aging patterns of shape and the corresponding texture in 3D domain by adapting a 3D morphable model to the 2D aging database (public domain FG-NET). At recognition time, each probe and all gallery images are modified to compensate for the age-induced variation using an intermediate 3D model deformation and a texture modification, prior to matching. The proposed approach is evaluated on a set of age-separated probe and gallery data using a state-of-the-art commercial face recognition engine, FaceVACS. Use of 3D aging model improves the rank-1 matching accuracy on FG-NET database from 28.0% to 37.8%, on average.

1. Introduction

Law enforcement agencies have built, over time, very large databases of facial images of offenders. Digital face images are becoming prevalent in government issued documents (e.g., passports and driver licenses). This is due to the high compatibility of face biometric in machine readable travel document systems based on a number of evaluation factors among the six major biometric modalities [6]. The non-intrusiveness characteristic of face biometric often compensates for its relatively lower accuracy, which has made it popular in applications dealing with official documents. As a result, a number of critical security and forensic applications require automatic identification or verification capability based on facial images.

A major problem that various government and law enforcement agencies face is to detect "multiple enrollments" in the facial database that they maintain (such as mugshot, driver license photos or passport pictures). To address this problem, we need to develop face recognition systems invariant to images of the same user captured at different times. Many offenders will commit crimes at different periods in their lives, often starting as a young adult - or even before - and continue throughout their lives. It is not unusual to encounter a time difference of many years between enrollment and verification in some applications. Ling et al. [10] studied how age differences affect face recognition performance in a real passport photo verification task. Their results show that the aging process does increase the difficulty, but it does not surpass the influence of illumination or expression. However, as these latter issues, namely, illumination and expression, are being successfully addressed by incorporating 3D models, aging process will continue to be a major obstacle for performance improvement [20] [19].

The Face Recognition Grand Challenge (FRGC, 2006) evaluation showed that substantial progress has been made in face recognition [16]. Results of FRGC demonstrated that the performance improved by an order of magnitude over Face Recognition Vendor Test (FRVT 2002). However, automatic face recognition in unconstrained situations remains a challenging problem. The difficulties come from potentially large variations in face images from the same subject due to differences in pose, lighting, expression, age, and occlusion, leading to drastic performance degradation [11]. The FRVT report estimated a decrease in performance by approximately 5% for each additional year of age difference. Therefore, the development of age correction capability remains an important issue for robust face recognition.

The use of 3D face models and 3D range images has helped in achieving pose and expression invariance [11][13]. 3D face matching is intrinsically pose-invariant, and a deformable model can achieve robustness to expression variation. However, although range scanners and other 3D acquisition methods are becoming more accessible, it may not be feasible in the foreseeable future to replace existing mugshot capture systems by expensive 3D systems

978-1-4244-2154-1/08/$25.00

Table 1. A comparison of age modeling methods for face recognition.

	Approach	Face matcher	Database	Rank-1 identification accuracy (%)	
				before aging simulation	after aging simulation
Ramanathan et al. (2006) [20]	Shape growth modeling up to age 18	PCA	109 subjects in a private database	8.0	15.0
Lanitis et al. (2002) [8]	Build an aging function in terms of PCA coefficients of shape and texture	Mahalanobis distance between PCA coefficients	12 subjects in a private database	57.0	68.5
Geng et al. (2007) [5]	Learn aging pattern based on concatenated PCA coefficients of shape and texture across a series of ages	Mahalanobis distance between PCA coefficients	10 subjects in FG-NET	14.4	38.1
Wang et al. (2006) [24]	Build an aging function in terms of PCA coefficients of shape and texture	PCA	No. of subjects n/a; 2,000 images in a private database	52.0	63.0
Patterson et al. (2006) [14]	Build an aging function in terms of PCA coefficients of shape and texture	PCA	9 subjects in MORPH	11.0	33.0
Proposed method	Learning aging pattern based on PCA coefficients in separated shape and texture. Modeling in 3D domain given 2D database	FaceVACS	82 subjects in FG-NET	28.0	37.8

and to ask a user to provide 3D images both at enrollment and identification stages. A strategy involving matching 2D images to 3D models is more appropriate, where the 2D probe images are compared to 2D renderings of the gallery 3D model under varying pose, lighting condition and expression. Another possibility is to warp 2D probe images by 3D models fitted to those images, and then compare the warped images to 2D gallery images.

1.1. Related Work

Studies on face verification across age progression [19] have shown that: (i) simulation of shape and texture variations caused by aging is a challenging task, as factors like life styles and weather contribute to changes in addition to biological factors, (ii) the aging effects can be best understood using 3D scans of human heads, and (iii) the few existing aging databases are not only small but also contain uncontrolled external variations. Due to these reasons, the effect of aging in facial recognition has not been as extensively investigated as other factors of intra-individual variations in facial appearance. A few studies on aging process can be found in biological sciences, e.g. in [23, 18]. These studies have shown that cardioidal strain is a major factor in aging of facial outlines. Such results have also been used in psychological studies, e.g. introducing aging by caricatures generated by shifting 3D model parameters [12]. Patternson et al. [15] compared automatic aging simulation results with forensic sketches and showed that further studies in aging are needed to improve face recognition techniques. A few image-based approaches in 2D have already been proposed to simulate both growth and adult aging, e.g. [20, 22]. These seminal studies demonstrated the feasibility of improving face recognition accuracy by simulated aging. There are also some developments in the related area of age estimation using statistical models, e.g. [8, 7]. Geng et al. [5] propose to learn a subspace of aging pattern based on the assumption that similar faces age in similar ways. Their

face representation is composed of face texture and the 2D shape represented by the coordinates of the feature points as in Active Appearance Models. Table 1 gives a brief comparison of these aging methods where the performance is evaluated by the identification accuracy. When multiple accuracies are reported in any of the studies in the same experimental setup, average value is used for the comparison. In case multiple accuracies are derived from different approaches, the best performance is used for the comparison. The identification accuracies of various studies reported in the literature that are shown in Table 1 cannot be directly compared due to the differences in the database, number of subjects and the face recognition method. Usually, the larger the number of subjects and the larger the database variations in terms of age, pose, lighting and expression, the smaller the recognition performance. The identification accuracy for each approach in Table 1 before age simulation represents the difficulty of the experimental setup for the face recognition test as well as the capability of the face matcher.

1.2. Aging Database

There are two well known public domain face aging databases; FG-NET [1] and MORPH [21]. The FG-NET database contains 1,002 images of 82 subjects ($\sim$12 images/subject), with the minimum age being 0 ($<$ 12 months) and the maximum age being 69. The MORPH database contains 1,724 images of 515 subjects ($\sim$3 images/subject). Since it is desirable to have as many images as possible at different ages for each subject for the aging pattern modeling, FG-NET database is more useful for age simulation than MORPH. We have used the complete FG-NET database for aging model construction and used it in the leave-one-out fashion for recognition. Note that while Geng et al. [5] also used FG-NET, they used very small subsets of it with only 10 subjects in each. We have used all the 82 subjects in FG-NET for face recognition.

1.3. Contributions

We have developed a 3D deformation model for craniofacial aging, which is compatible with 3D model-assisted methods [13, 11] used for pose and expression invariance. This way, major factors influencing the face recognition performance (illumination, pose and aging) can be handled by a single framework. With the fitted 3D model, we can effortlessly establish the correspondence based on facial texture and incorporate texture in aging-simulation. Once the aging-simulated shape of a probe image is obtained, we can use the aging-simulated texture to render the age-adjusted face image.

2. Aging Model

We propose to create a 3D aging model suitable for the task of face recognition, since the true craniofacial aging model can be naturally formulated in 3D. With 2D projection, growth parameters for landmarks can only be estimated based on a limited number of facial proportions that can be reliably estimated from photogrammetry of frontal images. The proposed 3D model would allow us to incorporate texture into individual facial components such as eye, mouth, and forehead, which is in line with the aging simulation method based on a graph structure [22]. 3D models can also be used to locate muscle fibers, and wrinkles can be generated across and orthogonal to the fibers [9]. The general form of the model is a narrow furrow with a bulge that can be rendered using a modified texture or an additional bump map. The simulation of aging in the texture based on the analysis of muscle fiber structure is beyond the scope of this paper. However, we provide a straightforward image-based aging simulation for the texture.

2.1. 3D Model Fitting

Ideally, we would like to have high resolution 3D models at both enrollment stage and identification stage. However, the database FG-NET [1], only contains 2D images. Some of these images, especially those taken tens of years back, are of poor quality. To create coarse 3D models for the subjects at different ages before analyzing the 3D aging pattern, we fit a general model based on feature correspondences.

The morphable model used here is a simplified version of the Blanz and Vetter model [2]. We keep the same point to point correspondences, but reduce each face mesh to 81 vertices, including the 68 feature points used in FG-NET. The additional 13 feature points are used to delineate the contour of the forehead, which is inside the region used to generate the feature sets and the reference sets in FaceVACS.

Following [2], we perform a Principal Component Analysis on the simplified meshes represented by shape-vectors (S_i's) containing the X, Y, Z-coordinates of all the vertices, and get the mean shape $\bar{S}$, the eigenvalues λ_i's and eigenvectors s_i's of the shape covariance matrix. We use only the top m ($= 30$) eigenvectors, for efficiency and stability of the fitting performed on the possibly very noisy dataset. Any shape in the space can then be represented as

$$S_\alpha = \bar{S} + \sum_{i=1}^{m} \alpha_i s_i, \tag{1}$$

where α contains the coordinates of the shape in the PCA basis, and the covariance matrix for (α_i) is $diag[\lambda_i]$.

As the FG-NET database contains 68 feature points for each face, we use them for the construction of a 3D model in the above space instead of using the matching between a rendered image of the 3D model and the original photo. In

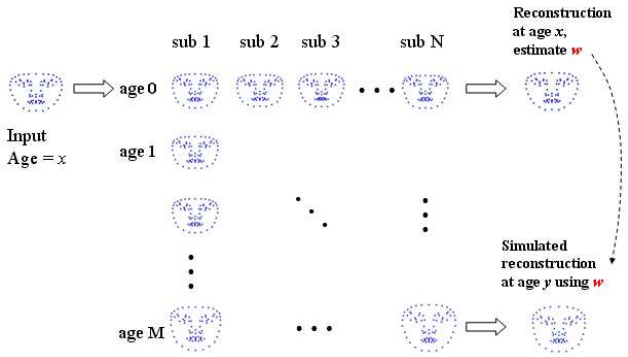

Figure 1. Aging simulation in 3D shape aging pattern space.

case we need to use other photos, we use Active Appearance Model [3] to extract the feature points as the input to the fitting algorithm.

To extract α_i's from a set of 68 2D points, we follow an iterative procedure similar to [17]. However, the deformable models we use are different as we are not tracking the motion of the face, but fitting a generic model to the feature set of a face projected to 2D. We assume the picture is taken at a distance much greater than the typical size of a human face, and thus we ignore the effect of perspective projection. Our goal is to find the minimizer (shape descriptor α_i, and rigid body transformations R and T) of the following target function

$$E = \sum_{i=1}^{n} (P(R(\bar{S} + \sum_{j=1}^{m} \alpha_j s_j) + T)_i - p_i)^2 / \sigma_N^2 + \sum_{j=1}^{m} \alpha_j^2 / \lambda_j, \tag{2}$$

where n is the number of 2D feature points p_i's, P is the projection matrix to $x - y$ plane, σ_N is the standard deviation of the estimated noise in the location of the 2D feature points, and the second term is a regularizer to control the Mahalanobis distance of the shape from the mean shape $\bar{S}$.

We initialize all the α_j's to 0, and the rotation matrix R is set to the Identity matrix. We then minimize E by alternately changing R and T with α_j fixed, and changing α_j with R and T fixed. Note that when both R and T are fixed, the target function E is a simple quadratic energy with Tikhonov regularization. There are multiple ways to estimate pose when we fix all the α_j's. Based on our tests, we found that first estimating the best 2×3 affine transformation $(P\ R)$ followed by a QR decomposition to get the best rotation works better than running a quaternion based optimization using Rodriguez's formula. Note that T_z is set to 0, as we use a simple orthogonal projection.

3. Aging Simulation

All 3D shapes are rescaled according to the anthropometric head width found in [4] to incorporate the global shape growth pattern. Then, our 3D shape pattern space is represented as a matrix of size M by N, where M is the number of different ages and N is the number of different subjects. Each element in the shape pattern space, S_i^j, is a vector representing the 3D shape of the subject i at age j generated by the procedure in Sec. 2. We use a simple interpolation to fill the missing values in the shape pattern space.

Given an unseen shape $S^{x,new}$ at age x, we can generate a weighted sum of the shapes at age x as

$$S^{x,new} = \bar{S^x} + \sum_{i=1}^{N} w_i^s (S_i^x - \bar{S^x}). \tag{3}$$

We again add a simple Tikhonov regularization term $\alpha^2 \sum_i w_i^2$ to the sum of the squares of the residuals, to resolve the case when there are multiple solutions for the weight vector $w^s = \{w_1^s, w_2^s, ..., w_N^s\}$ and the case when $S^{x,new}$ does not lie in the space spanned by the S_x^i's. Then we can generate a synthetic shape $S_{y,new}$ at an arbitrary age y using the weight vector w^s as

$$S^{y,new} = \bar{S^y} + \sum_{i=1}^{N} w_i^s (S_i^y - \bar{S^y}). \tag{4}$$

The texture pattern space is built independently of the shape. The full-filling of the texture aging pattern space and the simulation process are exactly the same:

$$T^{x,new} = \bar{T^x} + \sum_{i=1}^{N} w_i^t (T_i^x - \bar{T^x}), \tag{5}$$

$$T^{y,new} = \bar{T^y} + \sum_{i=1}^{N} w_i^t (T_i^y - \bar{T^y}), \tag{6}$$

where T_i^x is the texture of subject i at age x expressed in a global mean shape, and the weight vector w^t is independent of w^s. The aging simulation process for a new image at age x to age y is depicted in Figure 1. The pseudocode of shape aging pattern space construction and simulation are shown in Algorithms 3.1 and 3.2. The texture component follows the same steps.

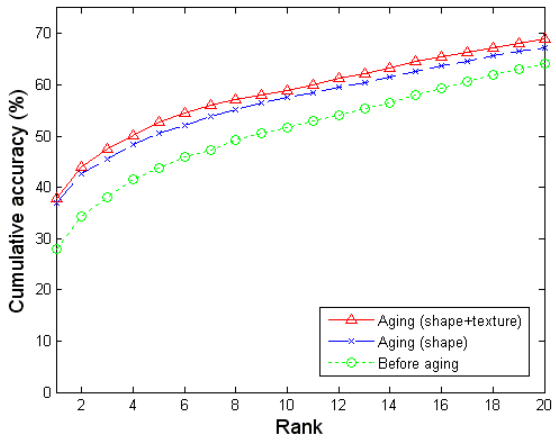

Figure 2. Cumulative Match Characteristic (CMC) curves before and after aging simulation in three different scenarios.

Algorithm 3.1: 3D SHAPE SPACE CONSTRUCTION( )

$Input: S_{2d} = \{s^1_{1,2d}, \ldots, s^j_{i,2d}, \ldots, s^M_{N,2d}\}$
$P = \{p^1_1, \ldots, p^j_i, \ldots, p^M_N\}$
$Output: S_{3d} = \{s^1_{1,3d}, \ldots, s^j_{i,3d}, \ldots, s^M_{N,3d}\}$
$T = \{t^1_1, \ldots, t^j_i, \ldots, t^M_N\}$
$i \leftarrow 1, j \leftarrow 1$
while $i < N$ & $j < M$
do
- **if** $s^j_{i,2d}$ is available
  - $k \leftarrow 1, e \leftarrow$ fitting error between $s^j_{i,2d}$ and $s^j_{i,3d}$
  - **while** $k < \tau$ & $e < \theta$
    - **do**
      - update pose (model param. fixed)
      - update model param. (pose fixed)
      - $k \leftarrow k + 1$, update e
  - construct $s^j_{i,3d}$ using pose and model param.
  - construct t^j_i using shape, pose and photop^j_i.

$i \leftarrow 1, j \leftarrow 1$
while $i < N$ & $j < M$
do
- **if** $s^j_{i,3d}$ is not available
- Fill $s^j_{i,3d}$ and t^j_i using interpolation

Algorithm 3.2: AGING SIMULATION ( )

$Input: S_{3d} = \{s^1_{1,3d}, \ldots, s^M_{N,3d}\}, S^{x,new}$
$Output: S^{y,new}$
Estimate w^s by $Eq.(3)$
Calculate $S^{y,new}$ by $Eq.(4)$

4. Performance Evaluation

We evaluate the performance of the proposed method by comparing the face recognition accuracy before and after aging simulation. We construct the probe data, $P = \{p^{x_1}_1, \ldots, p^{x_n}_n\}$, by selecting one image $p^{x_i}_i$ for each subject i at age x_i in the FG-NET database, $i \in \{1, \ldots, 82\}$, $x_i \in \{0, \ldots, 69\}$. The gallery data $G = \{g^{y_1}_1, \ldots, g^{y_n}_n\}$ is similarly constructed. The ages of probe data, x_i, are chosen as $X = \{0, 5, 10, \ldots, 30\}$ and the corresponding ages of gallery data, y_i, are chosen as $Y = \{x_i + 5, x_i + 10, \ldots, x_i + 30\}$. Note that for none of the subjects, images at all the ages in the range [0, 69] are available. Therefore, the closest possible ages of x_i and y_i to P and G, respectively, are selected with keeping $x_i \neq y_i$.

Let P, $P_{a,s}$ and $P_{a,st}$ be the probe, aging simulated probe using shape only and aging simulated probe using shape and texture, respectively. Let G, $G_{a,s}$ and $G_{a,st}$ be the gallery, aging simulated gallery using shape only and aging simulated gallery using shape and texture, respectively. All aging simulated images are generated in leave-one-out fashion using the shape and texture pattern space. Then the face recognition test is performed on the pairs P-G, $P_{a,s}$-$G_{a,s}$ and $P_{a,st}$-$G_{a,st}$. The identification rate for the probe-gallery pair P-G is the performance on original images. The accuracy of $P_{a,s}$-$G_{a,s}$ and $P_{a,st}$-$G_{a,st}$ are the performances after aging simulation. For the matching with aging simulation, we generated a symmetric transformation of $(x_i \rightarrow y_j)$ and $(y_j \rightarrow x_i)$ and the average matching score is used for the identification. We have observed that the combination of shape aging and shape+texture aging using score level fusion provide slightly better results. Score-sum based fusion with shape aging and shape+texture aging was used in our tests.

5. Results and Discussion

Fig. 2 shows the Cumulative Match Characteristic (CMC) curves before and after aging simulation. The improvement from aging simulation is more or less similar with those of other studies as show in Table 1. However, we have used FaceVACS, a state-of-the-art face matcher, which is known to be more robust against internal and external facial variations (e.g., pose, lighting, expression, etc) than the simple PCA based matcher. We believe the performance improvement using FaceVACS is more realistic than the performance improvement of PCA matcher. Fig. 3 shows the rank-one identification accuracies in each of the 42 different age pair groups of probe and gallery. The aging process can be separated as growth and development (age$\leq$18) and adult aging process (age$>$18). The face recognition performance is somewhat lower in the growth process where more changes occurs in the facial appearance. However, our aging process provides performance

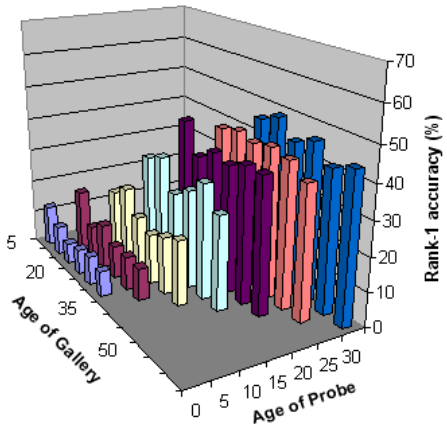

(a) Before Aging

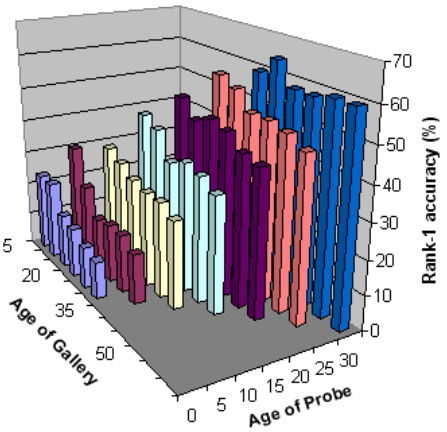

(b) After Aging (shape+texture)

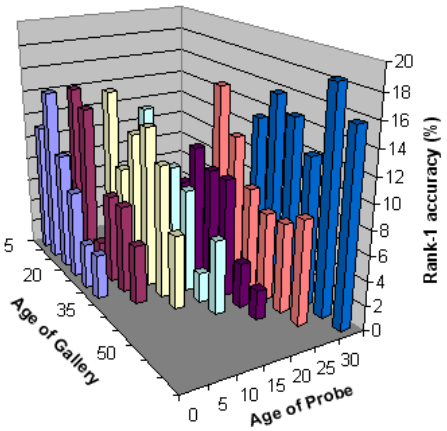

(c) Amount of improvement

Figure 3. Rank-one identification accuracies in each probe and gallery age groups: (a) before aging, (b) after aging and (c) amount of improvement after aging.

improvements in both age groups ≤ 18 and > 18. The average recognition results for age groups ≤ 18 are improved from 12.4% to 25.4% and those for age groups > 18 are improved from 42.3% to 53.1%.

Fig. 4 shows matching results for 7 subjects in FG-NET where the face recognition fails without age simulation but succeeds with age simulations for the first five subjects. The age simulation fails to provide correct matching for the last two subjects. For the first five subjects in Fig. 4 the probe and gallery images have similar shapes after the age simulation process. But, the probe and gallery images of the sixth subject are blurred and the probe image of the last subject shows distortion after pose correction and the gallery image contains severely different lighting condition. This is one of the reasons of failure in the matching even after aging simulation.

6. Conclusions and Future Work

We have proposed a 3D facial aging modeling and simulation method for aging-invariant face recognition. The extension of shape modeling from 2D to 3D domain gives additional capability of compensating for pose and lighting variations. The proposed age modeling method is capable of modeling the growth pattern as well as the adult aging. We have evaluated the proposed approach using a state-of-the-art commercial face recognition engine (FaceVACS), and obtained improvement in face recognition performance. We have shown that our proposed method is capable of handling both growth-and-development and adult face aging and provide performance. However, we have observed that in a small percentage of cases the proposed aging modeling causes failure of matching after the aging simulation. This shows the need to improve the proposed aging modeling technique. We plan to evaluate the proposed approach to a wider range of images, e.g., the MORPH database. We will also explore the optimal method for building aging pattern space given noisy 2D or 3D shape and texture data by cross validating the aging pattern space and aging simulation results in terms of face recognition performance.

Acknowledgments : This research project was partially supported by the NSF (CCF-0811313).

References

[1] FG-NET Aging Database, http://www.fgnet.rsunit.com.

[2] V. Blanz and T. Vetter. A morphable model for the synthesis of 3d faces. In *SIGGRAPH '99: Proc. 26th annual conference on Computer Graphics and Interactive Techniques*, pages 187–194, New York, NY, 1999.

[3] T. F. Cootes, G. J. Edwards, and C. J. Taylor. Active appearance models. *IEEE Trans. on Pattern Anal. and Mach. Intell.*, 23(6):681–685, 2001.

[4] L. G. Farkas, editor. *Anthropometry of the Head and Face*. Lippincott Williams & Wilkins, 1994.

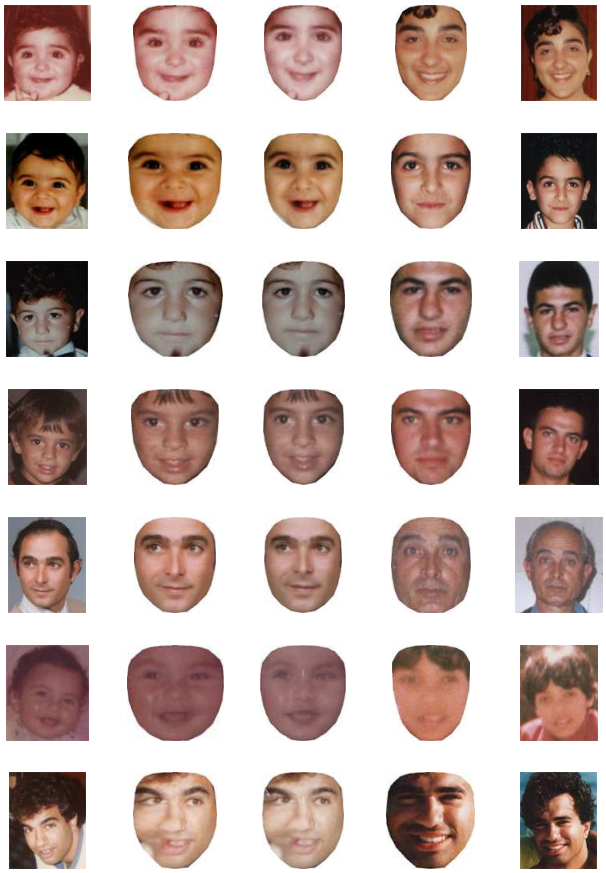

Figure 4. Example matching results before and after age simulation for seven different subjects: (a) probe, (b) pose-corrected probe, (c) age-simulated probe, (d) pose-corrected gallery and (e) gallery. All the images in (b) failed to match with the corresponding images in (d) but images in (c) were successfully matched to the corresponding images in (d) for the first five subjects. Matching for the last two subjects failed both before and after aging simulation. The ages of (probe, gallery) pairs are (0,18), (0,9), (4,14), (3,20), (30,54), (0,7) and (23,31), respectively, from the top to bottom row.

[5] X. Geng, Z.-H. Zhou, and K. Smith-Miles. Automatic age estimation based on facial aging patterns. *IEEE Trans. Pattern Anal. Mach. Intell.*, 29:2234–2240, 2007.

[6] R. Heitmeyer. Biometric identification promises fast and secure processing of airline passengers. *ICAO Journal*, 55(9), 2000.

[7] A. Lanitis, C. Draganova, and C. Christodoulou. Comparing different classifiers for automatic age estimation. *IEEE Trans. SMC-B*, 34(1):621–628, February 2004.

[8] A. Lanitis, C. J. Taylor, and T. F. Cootes. Toward automatic simulation of aging effects on face images. *IEEE Trans. Pattern Anal. Mach. Intell.*, 24(4):442–455, 2002.

[9] W.-S. Lee, Y. Wu, and N. Magnenat-Thalmann. Cloning and aging in a vr family. In *VR '99: Proc. IEEE Virtual Reality*, page 61, Washington, D.C., 1999.

[10] H. Ling, S. Soatto, N. Ramanathan, and D. Jacobs. A study of face recognition as people age. In *IEEE International Conference on Computer Vision (ICCV)*, 2007.

[11] X. Lu and A. K. Jain. Deformation modeling for robust 3d face matching. In *IEEE Conf. Computer Vision and Pattern Recognition (CVPR)*, pages 1377–1383, Washington, D.C., 2006.

[12] A. OT'oole, T. Vetter, H. Volz, and E. Salter. Three-dimensional caricatures of human heads: distinctiveness and the perception of facial age. *Perception*, 26:719–732, 1997.

[13] U. Park, H. Chen, and A. K. Jain. 3d model-assisted face recognition in video. In *CRV '05: Proc. 2nd Canadian Conference on Computer and Robot Vision*, pages 322–329, Washington, D.C., 2005.

[14] E. Patterson, K. Ricanek, M. Albert, and E. Boone. Automatic representation of adult aging in facial images. In *IASTED '06: Proc. 6th International Conference on Visualization, Imaging, and Image Processing*, pages 171–176, 2006.

[15] E. Patterson, A. Sethuram, M. Albert, K. Ricanek, and M. King. Aspects of age variation in facial morphology affecting biometrics. In *BTAS '07: Proc. First IEEE International Conference on Biometrics: Theory, Applications, and Systems*, pages 1–6, 2007.

[16] P. J. Phillips, W. T. Scruggs, A. J. O'Toole, P. J. Flynn, K. W. Bowyer, C. L. Schott, and M. Sharpe. FRVT 2006 and ICE 2006 Large-Scale Results. Technical Report NISTIR 7408, National Institute of Standards and Technology.

[17] F. Pighin, R. Szeliski, and D. H. Salesin. Modeling and animating realistic faces from images. *Int. J. Comput. Vision*, 50(2):143–169, 2002.

[18] J. B. Pittenger and R. E. Shaw. Aging faces as viscal-elastic events: Implications for a theory of nonrigid shape perception. *J. Exp. Psych.: Human Perception and Performance*, 1:374–382, 1975.

[19] N. Ramanathan and R. Chellappa. Face verification across age progression. In *IEEE Conf. Computer Vision and Pattern Recognition (CVPR)*, volume 2, pages 462–469, 2005.

[20] N. Ramanathan and R. Chellappa. Modeling age progression in young faces. In *IEEE Conf. Computer Vision and Pattern Recognition (CVPR)*, volume 1, pages 387–394, 2006.

[21] K. J. Ricanek and T. Tesafaye. Morph: A longitudinal image database of normal adult age-progression. In *FGR '06: Proc. 7th International Conference on Automatic Face and Gesture Recognition*, pages 341–345, Washington, D.C., 2006.

[22] J. Suo, F. Min, S. Zhu, S. Shan, and X. Chen. A multi-resolution dynamic model for face aging simulation. In *IEEE Conf. Computer Vision and Pattern Recognition (CVPR)*, 2007.

[23] D. W. Thompson. On Growth and Form. *New York: Dover*, 1992.

[24] J. Wang, Y. Shang, G. Su, and X. Lin. Age simulation for face recognition. In *ICPR '06: Proc. 18th International Conference on Pattern Recognition*, pages 913–916, 2006.